J Nanostruct 13(1): 238-253, Winter 2023

RESEARCH PAPER

Preparation and Characterization of Modified Release Nanoparticles Containing Cloperastine Hydrochloride Using Solvent Evaporation Method

Muath Sheet Mohammed Ameen

Department of Pharmacy, College of Pharmacy, Knowledge University, Erbil, Iraq

ARTICLE INFO

Article History:
Received 02 October 2022
Accepted 28 December 2022
Published 01 January 2023

Keywords:
Cloperastine hydrochloride
Emulsion solvent evaporation
HPC
HPMC
Prolonged-release
Nanoparticles

ABSTRACT

The goal of this study is to design prolonged-release Cloperastine hydrochloride nanoparticles. The emulsion solvent evaporation method was used to produce the nanoparticles made from polymers, such as hydroxypropyl methylcellulose K4M, hydroxypropyl cellulose, xanthan gum, chitosan, and sodium alginate. Scanning electron microscopy and transmission electron microscopy were used to evaluate the morphological characteristics of the resultant nanoparticles. The particle size, zeta potential, and polydispersity index of nanoparticle formulations were determined using photon correlation spectroscopy. The drug loading efficiency and drug release profiles of drug-containing formulations were studied by the HPLC method. The prepared formulations exhibited nanoscale particle sizes in the range of 19.74±0.73-49.26±0.25 nm and narrow polydispersity indexes in the range of 0.42±0.02-0.97±0.01. The zeta potential values of the formulations with different compositions were found in the range of -15.21±0.03 to -29.49±0.08, indicating the higher stability of the prepared nanoparticles. In addition, high yield percentage, drug entrapment efficiency, and drug loading values of 94.76±0.37%, 90.52±0.24, and 89.96±0.22 were obtained for the prepared formulations, respectively. According to the results, the formula comprising HPMC K4M and HPC showed highly effective physicochemical and functional properties and released more than 70% of the Cloperastine HCL after 8 hours in drug release studies. The results of this study confirmed that the individual and composite forms of natural polymers in the studied ratio could control the release of Cloperastine hydrochloride and could be used as effective nanoparticulate formulations for controlled release drug delivery of Cloperastine hydrochloride.

How to cite this article
Mohammed Ameen M s. Preparation and Characterization of Modified Release Nanoparticles Containing Cloperastine Hydrochloride Using Solvent Evaporation Method. J Nanostruct, 2023; 13(1):238-253. DOI: 10.22052/JNS.2023.01.025

INTRODUCTION

The usage of respiratory medications has risen in recent years due to the predominance of the Coronavirus disease 2019 (COVID-19) and its associated consequences [1, 2]. Cloperastine is a cough reliever that has been licensed for use in respiratory illnesses, such as colds, acute bronchitis, chronic bronchitis, bronchiectasis, tuberculosis, and lung cancer. Furthermore, Cloperastine is generally accepted as a non-specific antiviral agent, which can be beneficial in controlling and managing COVID-19 infection

* *Corresponding Author Email: maad2007@gmail.com*

This work is licensed under the Creative Commons Attribution 4.0 International License.
To view a copy of this license, visit http://creativecommons.org/licenses/by/4.0/.

and its associated symptoms [3, 4]. As a result, the impact of Cloperastine on COVID-19 was investigated in clinical studies to assess the effect of medication exposure in comparison to some of the prospective medicines used to treat COVID-19. Some medications, such as Clemastine, Cloperastine, Haloperidol, Hydroxychloroquine, and Zotatifin, have been shown to be beneficial in treating COVID-19 by inhibiting virus-host interactions via protein inhibition [5]. Despite the fact that immunizations were given in most countries, the diseases will be seasonal. Consequently, Cloperastine will remain beneficial in the treatment of cough in such diseases.

Cloperastine hydrochloride is a central antitussive having a comparable antihistaminic action as codeine but without the narcotic effect. This compound has been proven in trials to work on the center of cough in the brain without disrupting the center of respiration [4]. Furthermore, Li B et al. discovered that Cloperastine could suppress esophageal squamous cell carcinoma proliferation in a xenograft mice model by inhibiting oxidative phosphorylation in mitochondria [6]. Cloperastine hydrochloride belongs to the class of organic compounds known as diphenylmethanes and is chemically defined as 1-(2-((4-Chlorophenyl) (phenyl)methoxy)ethyl)piperidine hydrochloride (Fig. 1.). It is a white powder that easily dissolves in water, methanol, ethanol, acetic acid, and acetic anhydride [7].

The therapeutic dose of Cloperastine is three times a day for adults, 10–20 mg each time. It takes effect after 20–30 min, and the single-dose administration lasts 3–4 h [3]. After rapid oral absorption, it reaches peak concentration at 1–1.5 h, $t_{1/2}$ was 23.0 ± 7.7 h, and $AUC_{0-\infty}$ was 81.0 ± 46.9 h·ng/ml [8]. It is metabolized in the liver and eliminated by the kidneys and bile within 24 h of administration [9, 10]. However, some adverse effects, such as sedation, drowsiness, heartburn, and thickening of bronchial secretions were reported following Cloperastine administration [3]. Furthermore, the rapid release, absorption, and clearance of Cloperastine resulted in required frequent drug administration, which led to strong side effects and low patient compliance. Therefore, major efforts have been established to develop sustained-release formulations of Cloperastine to decrease its administration frequency, metabolism, and side effects [11-13]. In this regard, nano-based technologies in the form of nanoparticles, nanocarriers, nano-scaffolds, etc., have been attracted a great deal of interest to incorporate and deliver different therapeutical agents in order to enhance their therapeutical efficiency and diminish their various side- and adverse effects[14-16].

Among the various nano-based systems, nanoparticulate formulations in the form of solid, hollow, and core-shell nanoparticles have been applied widely for incorporating and delivering various pharmaceutically active agents (API) in treating different diseases and illnesses [16-18]. These systems are generally developed from synthetic and naturally-origin polymeric

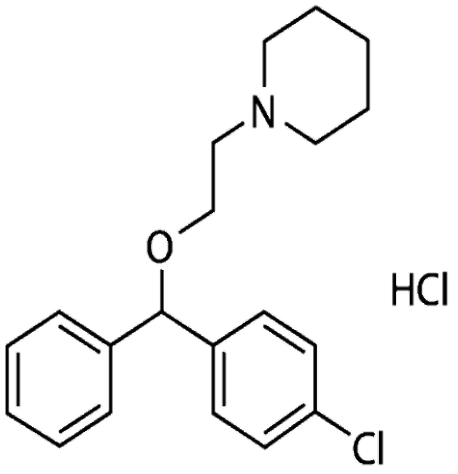

Fig. 1. The chemical structure of Cloperastine hydrochloride.

CC BY

or non-polymeric materials and offer many advantageous properties, such as biodegradability, biocompatibility, inertness, lower cytotoxicity, etc., toward application in biomedical and pharmaceutical applications [19, 20]. Among various types of nanoparticles, polymeric nanoparticles (PNPs) have recently attracted a significant deal of interest because of their distinctive characteristics, such as their diminutive size, suitable zeta potential, biosafety, etc. These nanoparticulate materials have the ability to be used in various applications, including medication delivery and diagnostics [21, 22]. Advantages of PNPs as carriers can protect and precisely target drug molecules, allowing for enhancements to the therapeutic index and the achievement of controlled release behavior [23-25].

Accordingly, the present study aimed to develop an effective formulation of Cloperastine hydrochloride nanoparticles with a prolonged release profile. To achieve this goal, a number of water-soluble polymers were utilized, and the preparation was conducted using the solvent evaporation method. The drug concentration, entrapment efficiency, zeta potential, particle size, in-vitro release rate, and morphology of the resulting formulations were examined. Among the different prepared formulations, the formula (CHMH2) displayed excellent zeta potential, desired nanoparticle morphology, and sustained release profile for controlled oral delivery that surpasses 80% of Cloperastine hydrochloride after 8 h and lasts for 24 h.

MATERIALS AND METHODS

Materials

Cloperastine hydrochloride was purchased from BLD Pharmatech Ltd., China. Hydroxypropyl methylcellulose (HPMC K4M, medium molecular weight), chitosan (medium molecular weight), sodium alginate, xanthan gum, and hydroxypropyl cellulose (HPC, medium molecular weight) were bought from Sigma-Aldrich, USA. Acetone and acetonitrile were acquired from Merck, Germany. Acetonitrile for HPLC was ordered from E. Merck, Darmstadt, Germany. Hydrochloric acid, potassium dibasic phosphate, potassium monobasic phosphate, and sodium hydroxide pellets were purchased from Schuarlo, Spain. The preparation of pure water was done with a Milli-Q

Table 1. The amounts of various polymers used in the formulation of Cloperastine hydrochloride nanoparticles.

Formula	Chitosan (mg)	HPC (mg)	HPMC K4M (mg)	Sodium alginate (mg)	Xanthan gum (mg)
CC1	50				
CC2	100				
CC3	150				
CH1		50			
CH2		100			
CH3		150			
CHM1			40		
CHM2			60		
CHM3			80		
CHMH1		50	40		75
CHMH2		100	60		
CHMH3		100	80		
CS1				50	
CS2				100	
CS3				150	
CCS1	50			50	
CCS2	100			75	
CCS3	150			100	
CX1					40
CX2					60
CX3					80
CHMX1			40		40
CHMX2			60		60
CHMX3			80		80

CC BY

purification device.

Methods

Preparation of nanoparticles

The preparation of nanoparticles was conducted by the solvent evaporation method as reported in previous studies [26,28]. First, 200 mg of Cloperastine was dissolved in 25 ml of acetone and sonicated to create a clear solution. Various proportions of polymers, according to Table 1, were dissolved in 50 ml of water. Then, the drug solution was poured portionwise into 50 ml of the dissolved polymer while continuously stirring at 5000 rpm for 15 minutes using a homogenizer. Tween 80 (1g) was dissolved in 100 ml of liquid paraffin before being introduced dropwise to the drug-containing polymeric solution over the course of four hours with constant stirring. The resultant dispersion was centrifuged for 20 minutes at 16,000 rpm. The washing of the resultant particles was performed with 10 ml of acetone, 10 ml of ethanol, and 10 ml of water, then dried and stored.

Characterization of nanoparticles

Scanning electron microscopy (SEM)

The particle size and morphological characteristics of chosen Cloperastine HCL-containing nanoparticles were studied using the SEM technique (SEM-Jeol JSM 6460LV instrument). For this purpose, the dried formulations were placed on an SEM holder and coated with a thin layer of gold using a gold sputter unit in a high-vacuum evaporator. These samples were then observed by the SEM instrument, and photomicrographs were taken at an acceleration voltage of 10 kV [29].

Transmission electron microscopy (TEM)

The TEM experiments were also conducted to support the DLS data and provide information on the particles morphology. The TEM micrographs of the chosen sample were obtained using a JEM-2100 electron microscope (JEOL, Japan).

Particle size and zeta potential

The physicochemical properties of the formulation, such as surface charge and particle size also investigated by DLS and zeta potential measurements. For this purpose, the Cloperastine nanoparticle's stability and size homogeneity were examined within the prepared colloidal system. The zeta potential and particle sizes of Cloperastine nanoparticles were evaluated using photon correlation spectroscopy and a Zetasizer 3000HS (Malvern Instruments, UK). Every specimen was examined thrice after being diluted with deionized filtered water. The results are provided as the mean standard deviation (± SD).

Production yield, drug content, and entrapment efficiency

The production yield (%) of the nanoparticles was determined by comparing the nanoparticles mas obtained from centrifuging at 16,000 rpm and 20 minutes with the theoretical amount of materials initially used for their synthesis. The drug content of the prepared nanoparticulate formulations was determined by a direct ingestion method. Briefly, 100 mg of nanoparticles were precisely weighed, crushed, and solubilized in 100 ml of phosphate buffer (pH 6.8), then agitated for 6 hours using a magnetic stirrer. 2 ml of the solutions were transferred to a 100 ml flask and diluted with acetonitrile before filtering through a 0.2 m filter and determining the percent of dissolved medication using the established HPLC technique. The following equations were used to calculate the production yield (%), drug content, and entrapment efficiency [30-32]:

$$Production\ yield\ (\%) = \frac{practical\ mass}{theoritical\ mass} \times 100$$

$$Drug\ content = \frac{calculated\ drug\ in\ nanoparticles}{total\ weight\ of\ nanoparticles} \times 100$$

$$Entrapment\ efficiency\ (\%) = \frac{amount\ of\ the\ drug\ found\ in\ the\ prepared\ formula}{theortical\ amount\ of\ added\ drug} \times 100$$

CC BY

Drug Release Studies (In Vitro Dissolution Test)

For in vitro drug release studies, the hard gelatin capsules were filled with produced particles, each equivalent to 10 mg of Cloperastine hydrochloride. These capsules were then subjected to a release profile study. The capsules were placed in the USP basket dissolving tester equipment type I, which was rotated at 50 rpm in 250 ml of phosphate buffer pH 6.8. At different pre-determined time intervals (0.5, 1, 2, 4, 6, 8, 10, 12, 16, 20, and 24 hours), samples of 5 ml aliquots were withdrawn from the release medium and compensated with the new medium to maintain sink conditions. The amount of Cloperastine that was released into release medium was measured and quantified using the established HPLC method.

Development of HPLC method

Cloperastine HCl concentrations were determined using a reverse-phase HPLC method as described earlier with minor modifications [33, 34]. A Luna C18 (5 cm, 25 cm, 4.6 mm) column was used to separate the samples. Cloperastine was detected using a photodiode array detector at a wavelength of 262 nm. The injection volume was 50 µl, and the mobile phase was 5 mM phosphate buffer 6.5: acetonitrile (60:40) at ambient temperature with a 1.2 ml/min flow rate. The linearity, residual standard deviation, limit of detection (LOD), and limit of quantitation (LOQ) were assessed and reported for the obtained data from HPLC analysis.

Statistical analysis

All data in the present study were reported as mean ± standard deviation (SD), and the significant differences between groups were determined by Student's t-test or one-way analysis of ANOVA. Each experiment was repeated at least three times, and the results are considered statistically significant when the P value is equal to one of the following amount, *$p < 0.05$, **$p < 0.01$, and ***$p < 0.001$. The data analysis software was GraphPad Prism® program (GraphPad Software, Inc., Boston, USA).

RESULTS AND DISCUSSION

For drug loading and drug release studies, first, the calibration curve of Cloperastine HCL was established by the HPLC method. For this purpose, different concentrations of nanoparticles were subjected to HPLC analysis, and the amount of Cloperastine was quantified by detection at a wavelength of 262 nm. System appropriateness criteria for Cloperastine HCL, such as tailing factor (T), capacity factor (k'), and plate count, which should not be less than 2000, were determined sequentially before injection of the samples [35]. The values obtained for the parameters all fell within the ranges as summarized in Table 2. Therefore, the HPLC method established in the present study could be applied successfully for quantifying Cloperastine HCL amount of nanoparticles in drug loading and release studies.

Fig. 2 shows the HPLC chromatogram of Cloperastine hydrochloride obtained following the injection of pure Cloperastine hydrochloride along with the 5 mM phosphate buffer 6.5: acetonitrile (60:40) at ambient temperature with a 1.2 ml/min flow rate. As we can see, the pure Cloperastine hydrochloride showed a sharp peak at approximately 4.329 minutes with 0.15 intensity.

The calibration curve of Cloperastine was established in phosphate buffer 6.5:acetonitrile (60:40) at ambient temperature using different concentrations (40-120 µg/ml) and separately measuring the absorbance at λ = 262 nm. From Fig. 3, the linear regression of the calibration curve showed a good linear relationship over the studied concentration range of 0-4 µg/ml of Cloperastine. Table 3 summarizes the validation parameters that were performed in accordance with the ICH validation guideline [36] and USP methods [37]. The correlation coefficient (R^2) of the linearity of the established regression was greater than 0.999, which is well within the acceptable range and indicative linearity of the

Table 2. The suitability of the developed HPLC method.

Parameter	Criteria	Results
Theoretical plates number	≥ 2000	6000
Tailing factor	≤ 2	0.43
Capacity factor	≥ 2	6.40

CC BY

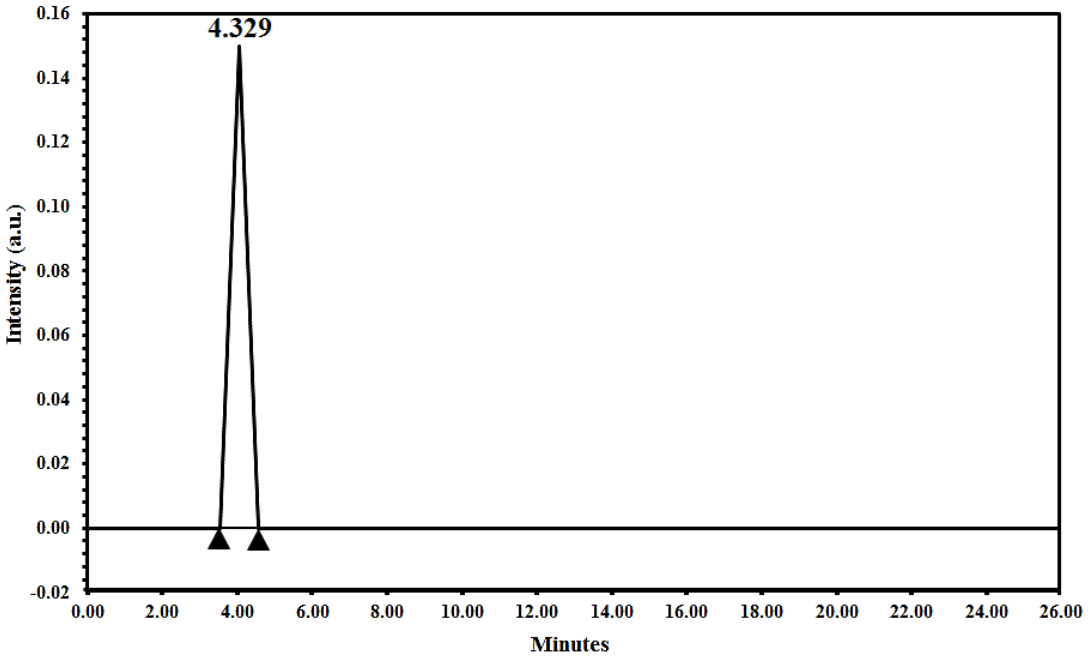

Fig. 2. HPLC chromatogram of Cloperastine hydrochloride.

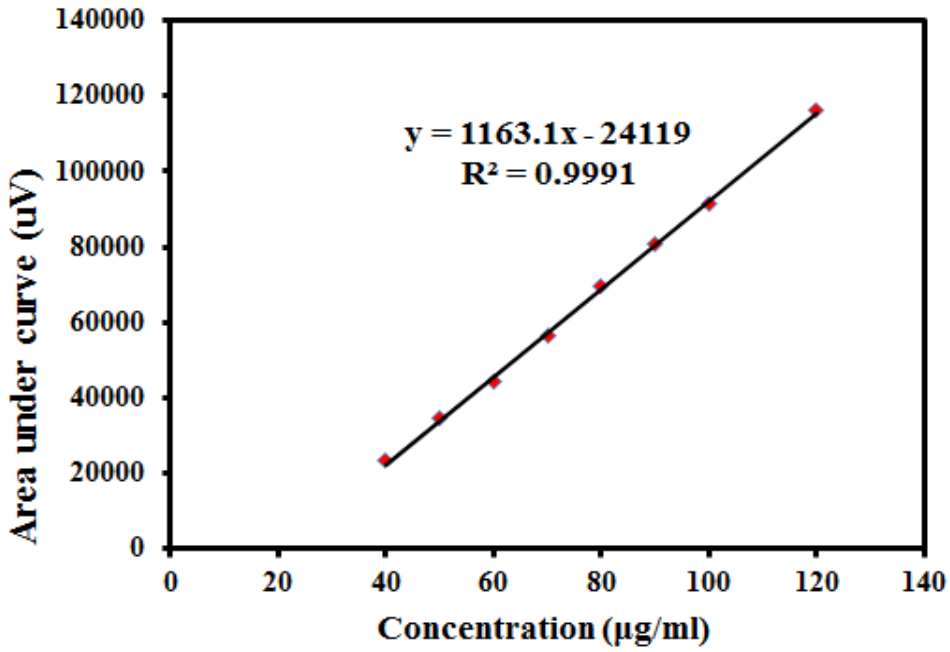

Fig. 3. Calibration curve of Cloperastine hydrochloride for the established HPLC method.

obtained equation. With a recovery between 98% and 102%, this technique is suitable for the quality control examination of pharmaceuticals. The precision of a technique is defined by the degree to which many measurements of the same sample are in agreement with one another [38]. The estimated RSD values were within the acceptable range of 2%, demonstrating the high precision of

CC BY

Table 3. Validation parameters of analytical method.

Parameter		Cloperastine
Linearity	Correlation coefficient R^2	0.9991
	Slope	-24119
	Intercept	1163.1
Accuracy	Mean % recovery± SD	99.85 % ± 0.27
Precision	Intraday (RSD %)	0.26
	Interday (RSD %)	0.18
Sensitivity	LOD	1.32 µg/ml
	LOQ	4.01µg/ml
Specificity	Recovery % (0.1 N HCl)	91.63 % ± 0.71
	Recovery % (0.1 N NaOH)	89.87 % ± 0.24
	Recovery % (10% H_2O_2)	90.16 % ± 0.43
Robustness	pH 6.2 (RSD%)	0.39
	RSD% at (pH 6.7)	0.17
	RSD% at 1.4 mL/min	0.35
	RSD% at 1 mL/min	0.42

the derived equation. Using GraphPad InStat®, the LOD and LOQ of Cloperastine regression were 1.32 µg/ml and 4.01 µg/ml, respectively [35]. These values represent the good sensitivity of the established method. Therefore, according to the experimental data represented and after statistical analysis, the established method in the present study is precise, accurate, and sensitive within the studied range.

The previously established HPLC method was employed to evaluate the amount of Cloperastine hydrochloride entrapped into the prepared nanoparticles and to study the drug release behavior of the developed formulations. In this study, Cloperastine hydrochloride was added to different polymeric formulations; all were then formed into nanoparticles. According to Table 4, a high %yield was observed with a minimum of 83.00 ± 0.19% in the case of CCS2 and CHMX3 and increased for the other formulations to 94.76 ± 0.37% for CS2 formulation. Except for HPMC K4M and HPC-containing formulations, the nanoparticle production yields remained almost constant by increasing the polymer content in all formulations. In the case of HPMC K4M and HPC-containing formulations (CH1-3, CHM1-3 and CHMX1-3), the production yield decreased following the increase in the respective polymer concentration. Moreover, the addition of HPMC K4M to xanthan gum formulations decreased the production yield. Similar results were identified through chitosan addition to alginate formulations, in which the production yield of nanoparticles decreased upon chitosan addition. These results confirmed the effectiveness of the established preparation method (solvent evaporation method) in the production of drug-containing polymeric nanoparticles. The %DL of the nanoparticulate formulations also showed higher values for all prepared formulations. In this regard, drug content (%DL) of the prepared nanoparticles ranged from 76.35% to 89.96% for all prepared formulations and a maximum value was obtained for CHMH2 formulation. On the other hand, the %DL of chitosan (CC1-3) and xanthan gum (CX1-3)-containing formulations were increased by increasing the polymer concentration, while the %DL of other formulations decreased slightly by increasing the polymer content of formulations. These results could be attributed to the higher

CC BY

viscosity and gel-forming capability of chitosan and xanthan gum compared to cellulosic and sodium alginate-based formulations, which effectively incorporate the drug within their gel-like and three-dimensional (3D) structures [39]. The %EE analysis of the prepared nanoparticles also produced high values for all formulations and a maximum %EE for CHMH2 formulation. In contrast with %DL results, the %EE of all formulations increase by increasing the formulation's polymer content. These results could also be attributed to the gel-forming characteristics of the formulations and abundant functional groups of the polymers, which encourage the polymer-drug interaction and enhance the %EE of all formulations with polymer content [40]. By evaluating the %yield, %DL, and %EE results of all formulations summarized in Table 4, it is clear that the CHMH2 formulation resulted in the highest production yield and drug incorporation efficiency.

Table 4. Mean particle size, %yield value, entrapment efficiency, zeta potential and mean particle size and PDI of nanoparticles.

Formula	Drug Loading* (DL%) ± SD	Production Yield* (%) ± SD	Entrapment efficiency (%EE)*	Zeta Potential* (mV) ± SD	Mean particle size* (nm) ± SD	Polydispersity index (PDI)*
CC1	78.25±0.36	80.49±0.24	72.57±0.36	-18.69±0.06	33.01±0.43	0.52±0.02
CC2	79.81±0.12	82.12±0.29	77.41±0.24	-20.12±0.08	35.25±0.39	0.97±0.01
CC3	81.42±0.27	81.33±0.37	78.47±0.33	-19.93±0.11	29.64±0.25	0.64±0.01
CH1	87.12±0.43	89.50±0.19	78.2±0.36	-15.21±0.03	21.42 ±0.24	0.56±0.02
CH2	76.35±0.24	83.92±0.34	79.41±0.24	-16.69±0.06	24.56±0.26	0.66±0.01
CH3	83.96±0.26	84.02±0.23	81.47±0.33	-18.15±0.08	19.74±0.73	0.90±0.01
CHM1	86.89±0.31	91.00±0.24	82.47±0.31	-18.24±0.11	34.21±0.47	0.46±0.02
CHM2	89.50±0.19	83.02±0.21	84.12±0.22	-19.54±0.03	25.47±0.29	0.52±0.01
CHM3	82.69±0.27	86.99±0.41	79.49±0.15	-20.69±0.09	29.39±0.35	0.50±0.01
CHMH1	87.21±0.37	91.26±0.28	86.75±0.47	-26.56±0.04	24.18±0.43	0.44±0.03
CHMH2	89.96±0.22	91.14±0.19	90.52±0.24	-29.49±0.08	20.14±.36	0.42±0.02
CHMH3	88.56±0.10	88.02±0.24	89.27±0.29	-26.97±0.05	29.47±0.49	0.49±0.01
CS1	89.45±0.32	93.41±0.22	73.41±0.24	-20.46±0.08	22.78±0.17	0.57±0.05
CS2	87.89±0.12	94.76±0.37	75.47±0.33	-21.69±0.10	25.69±0.33	0.88±0.01
CS3	86.99±0.33	93.56±0.23	82.47±0.20	-21.65±0.12	29.48±0.15	0.45±0.03
CCS1	88.56±0.15	86.00±0.31	80.51±0.27	-16.46±0.08	42.74±0.73	0.49±0.02
CCS2	89.45±0.32	83.00±0.19	81.27±0.29	-18.69±0.27	39.21±0.47	0.47±0.01
CCS3	85.41±0.15	85.02±0.24	84.9±0.31	-20.65±0.32	41.47±0.29	0.52±0.05
CX1	86.62±0.33	85.24±0.23	69.43±0.22	-17.34±0.41	42.39±0.48	0.77±0.01
CX2	88.14±0.27	84.00±0.15	72.49±0.33	-18.92±0.24	49.26±0.25	0.49±0.03
CX3	89.45±0.30	86.02±0.20	73.41±0.24	-18.61±0.19	40.57±0.37	0.45±0.02
CHMX1	87.89±0.18	91.15±0.23	75.47±0.33	-20.46±0.23	38.74±0.49	0.45±0.03
CHMX2	85.19±0.41	88.00±0.31	82.47±0.21	-21.64±0.36	36.68±0.18	0.69±0.02
CHMX3	82.56±0.25	83.00±0.19	83.51±0.27	-21.38±0.46	39.57±0.33	0.47±0.04

*Values revealed as mean ± standard deviation (SD), n=3.

CC BY

The particle size, zeta potential, and PDI values of the prepared nanoparticles were also determined by photon correlation spectroscopy and a zetasizer, and the results are represented in Table 4. The results showed particle sizes of 19.74 ± 0.73 to 49.26 ± 0.25 nm for all prepared formulations. Moreover, increasing the polymer concentration did not show an specific trend. However, for most formulations, the particle size initially increased and then decreased by increasing the polymer concentration. It is evident that the nanoparticles obtained from chitosan, xanthan gum, and HPMC K4M produced larger particle sizes, while HPC and alginate nanoparticles showed smaller sizes. Particle sizes of formulas containing chitosan and HPC decreased and of formulas containing HPMC K4M, sodium alginate, and xanthan gum increased when increased polymer contents. The particle sizes of formulas containing chitosan (CC1-3) and sodium alginate (CCS1-3) increased by mixing of chitosan with sodium alginate in CS1-3) formulas. Moreover, the addition of HPMC K4M to HPC formulations in CHMH2-3 and to xanthan gum formulations in CHMX1-3 caused increased the particle sizes of HPC content formulas (CH1-3) and decreased the particle sizes of xanthan gum content formulas (CX1-3). It is worth mentioning that all formulations produced particles in the nanoscale size, which confirms the suitability of the solvent evaporation method in the designing and fabrication of drug-loaded organic nanoparticles for pharmaceutical applications. Among all formulations, CH3 (19.74 ± 0.73) and CHMH2 (20.14 ± 0.36) formulations produced smaller nanoparticles, which could be considered effective formulations for pharmaceutical and biomedical applications. It is reported that the smaller particles are more appropriate for drug delivery of different drug agents to potentially enhance their therapeutic efficacy [41, 42].

The surface zeta potential of the formulations was also determined by the zetasizer, which is generally used as a suitable indicator for evaluating the physical stability of colloidal dispersion (Table 4). The zeta potential values of polymeric nanoparticles loaded with Cloperastine hydrochloride ranged from -15.21 ± 0.03 to -29.49 ± 0.08 mV. Except chitosan and xanthan gum formylations, the zeta potential of all formulations decreased by increasing the polymer

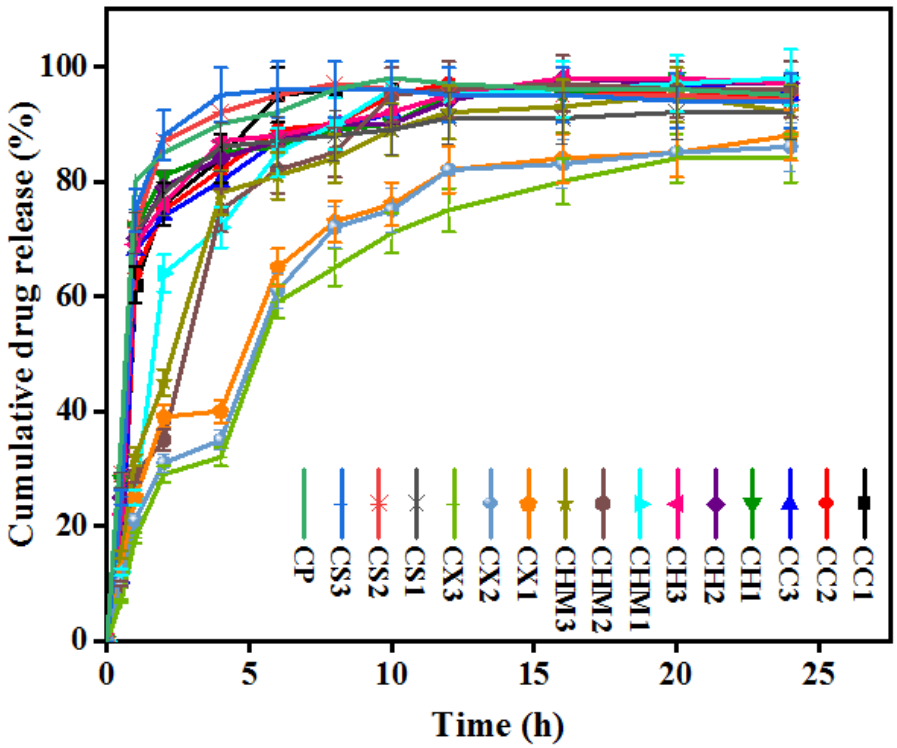

Fig. 4. Drug release profiles of the different single polymer formulations which compared with pure drug release profile (values revealed as mean ±SD, n=6).

CC BY

concentration. Although the polymer type did not significantly affect the zeta potential of different formulations, the lowest negative zeta potential was obtained for the CHMH2 formulation (-29.49 ± 0.08 mV). The negative surface charge of organic nanoparticles with the same composition was also reported in previous studies and might be attributed to the presence of hydroxyl groups of the polymers used in the formulations [43-46]. However, the zeta potential of chitosan-containing formulations showed contradictory results with the positive values reported in previous studies. This could be attributed to the un-protonated nature of these formulations, which were prepared in a very diluted acidic acid solution (1%). In fact, the acetic acid concentration in these formulations was not sufficient to protonate the chitosan's amine groups in order to produce positive zeta potentials. Therefore, the negative charge of the amine and hydroxyl groups resulted in a negative zeta potential for the resulting formulations. It is reported that zeta potential values over +30 mV and below -30 mV exert sufficient repulsive forces that result in better physical colloidal stability [47, 48]. Therefore, all prepared formulations in the present study possess effective surface charges to attain highly stable characteristics over long periods.

The polydispersity index (PDI) of the prepared nanoparticles is also determined by the DLS technique, and the results in Table 4 explained that all fabricated nanoparticles produced uniform particle sizes with narrower PDI values ranging from 0.42 ± 0.02 for CHMH2 formulation to 0.97 ± 0.01 for CC2 formulation. Comparing the PDI values of the various nanoparticles with different polymers revealed that similar to particle sizes results, the highest PDI values belong to chitosan, xanthan gum, and alginate-based nanoparticles. These results also could be related to the higher gel-forming capability of these polymers that largely swells in aqueous media and increase the PDI values of the resultant nanoparticles based on their initial particle sizes. In fact, in these formulations, the slight variation in particle size results in a significant increase in the PDI values. Therefore, the nanoparticles obtained from chitosan and alginate could be considered as hydrogelic nanoparticles. However, the overall PDI values of all formulations are still less than 1 and clearly indicate uniform particle size distributions for different prepared nanoparticles. Finally, among different formulations, the CHMH2 formulation showed enhanced physicochemical properties in terms of particle size, zeta potential, PDI, drug loading and drug entrapment efficiencies.

The *in vitro* release profile of Cloperastine hydrochloride from fabricated nanoparticles was studied under physiological conditions (phosphate buffer pH 6.8). All measurements were carried out in triplicate, and the mean of these three data was used to calculate the concentration of the drug released. According to Fig. 4-7, all prepared formulations, as well as pure Cloperastine, exhibited two-stage release behavior at the studied time period. First, a rapid release rate with a high burst of around 80% at 1-2 h was observed that then increased gradually and reached a steady state concentration with a complete release (100%) after 12 h. Fig. 4 shows the drug release profiles of the different single polymeric formulations compared with pure drug release profile. Pure Cloperastine hydrochloride showed the highest drug release content, especially at the initial times. However, except for the HPMC K4M and xanthan gum-containing formulations, the alginate, chitosan, and HPC-based formulations showed a similar trend of drug release profile with pure drug, indicating burst release behaviors of these formulations. Moreover, the variation of polymer contents in the cellulosic formulations did not affect the amount of drug released from the resultant nanoparticles. However, increasing alginate concentration in the related formulations increased the drug release amount, especially at lower concentrations. Contradictory results were obtained for chitosan formulations, in which the increase in chitosan concentration retarded the drug liberation. However, unlike other formulations, the xanthan gum nanoparticles exhibited the lowest drug liberation rate in the studied time period, suggesting their effective sustained release behavior. In this regard, the release of Cloperastine from the formulas containing chitosan (CC1, CC2, and CC3) was ≥ 80% after 4 h, while the formulas prepared with sodium alginate (CS1, CS2, and CS3) exhibited a release higher than 86% after 4 h. These results could be attributed to the higher and more effective interaction of Cloperastine hydrochloride with chitosan and xanthan gum's different functional groups. On the other hand, increasing the

CC BY

chitosan and xanthan gum concentration in these formulations decreased the drug release content and improved its sustained release behavior. This is very interesting because increasing the alginate concentration increases the drug release content, which again confirms that the drug release profile of the prepared nanoparticles determines by drug-carrier interactions and nanoparticles degradation behavior rather than passive diffusion mechanisms of the drug through polymeric matrices. In this regard, the chitosan and xanthan gum nanoparticles provide suitable interactions with Cloperastine hydrochloride and retard its liberation and dissolution in the release medium.

Fig. 5-7 shows the drug release profiles of the Cloperastine hydrochloride from the fabricated polymeric composite nanoparticles prepared by combining different polymeric materials. In these diagrams, the release profiles of single polymeric nanoparticles are compared with their composite forms and with the release profile of the pure drug. The combination of chitosan and alginate polymers in the form of nanoparticles decreased the release profile of the drug and produced a sustained release behavior. Therefore, chitosan-sodium alginate nanoparticles (CCS1, CCS2, and CCS3) showed a slower release (65%) after 4 h compared with their single composition formulations (CC1-3 and CS1-3). Similar results were also observed for the combination of the two cellulosic polymers. In this regard, HPC-based formulas (CH1, CH2, and CH3) released more than 90% of Cloperastine hydrochloride after 8 h, while HPC-HPMC K4M-containing formulas (CHMH1 and CHMH2) released more than 82% and 73% drug after this time. Therefore, the CHMH composite nanoparticles resulted in a sustained release profile compared with their single polymer formulations (CH and CHM nanoparticles). On the other hand, it is evident that increasing the HPC concentration in CH formulas decreased the released drug content in these formulations. However, the addition of HPMC to the xanthan gum formulations increased the drug release amount of the final formulations in a concentration-dependent manner. In this respect, the amount of Cloperastine HCL that

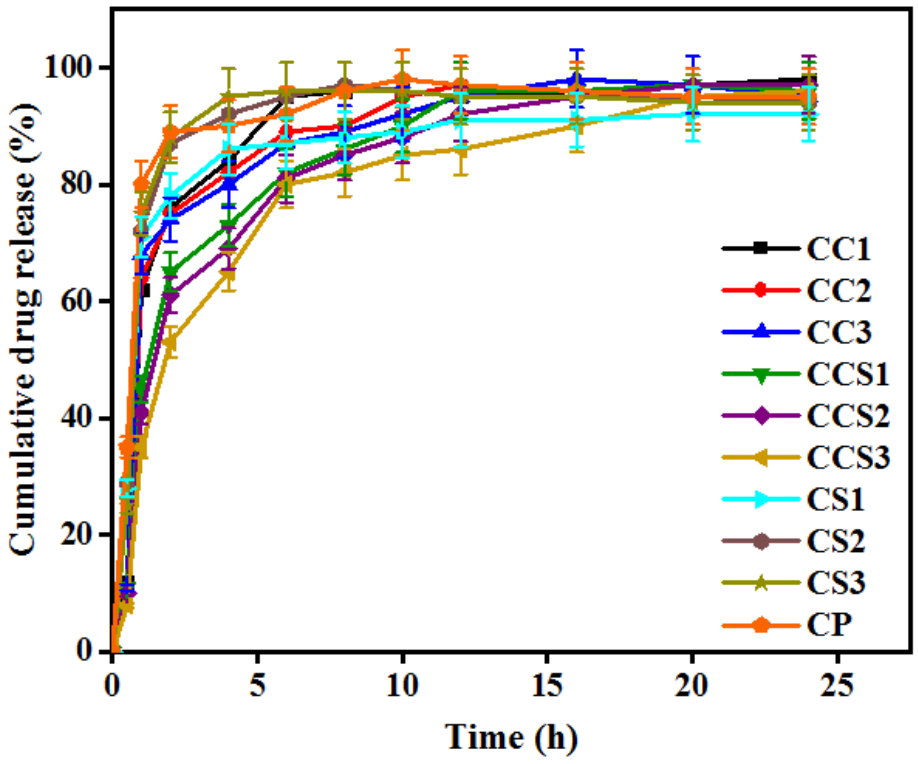

Fig. 5. Release rate of Cloperastine hydrochloride (CP) from chitosan, sodium alginate and chitosan/sodium alginate single and composite nanoparticles (values revealed as mean ±SD, n=6).

CC BY

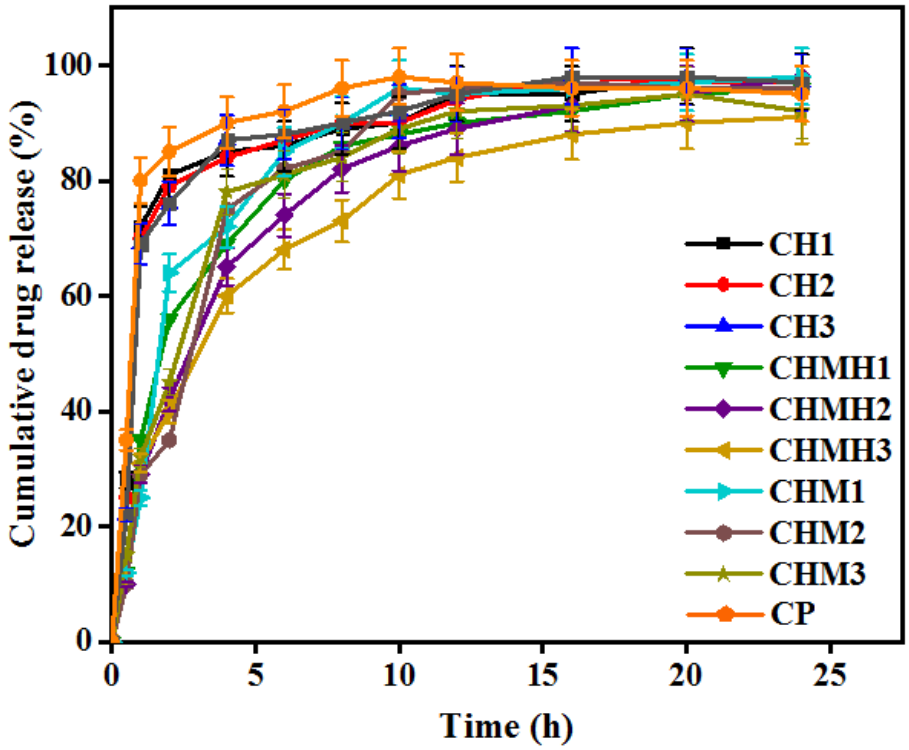

Fig. 6. Release rate of Cloperastine from HPC, HPMC K4M, and HPC/HPMC K4M single and composite nanoparticles (values revealed as mean ±SD, n=6).

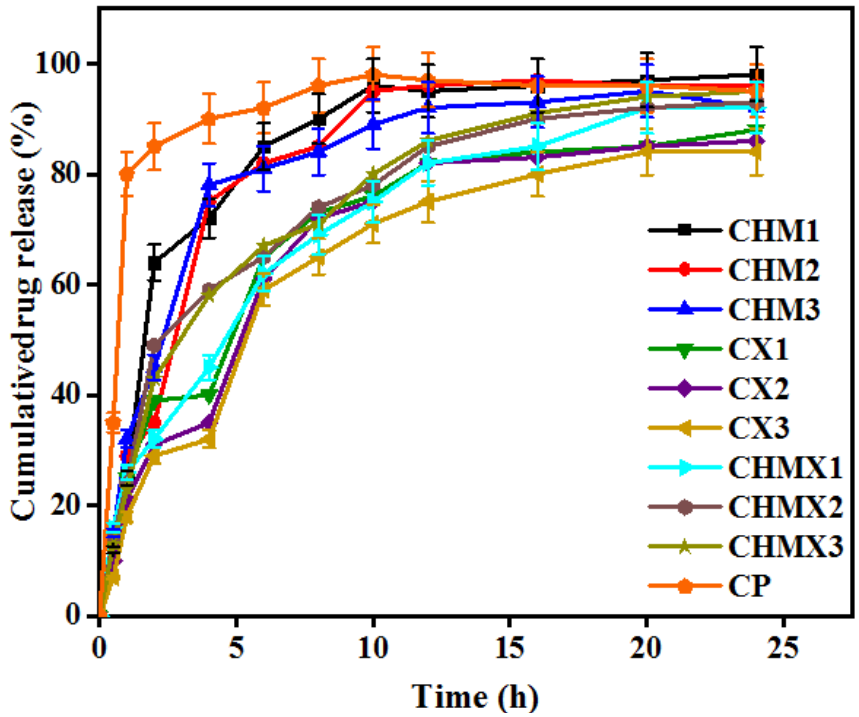

Fig. 7. Release rate of Cloperastine hydrochloride (CP) from HPMC K4M, xanthan gum, and HPMC K4M/ xanthan gum single and composite nanoparticles (values revealed as mean ±SD, n=6).

CC BY

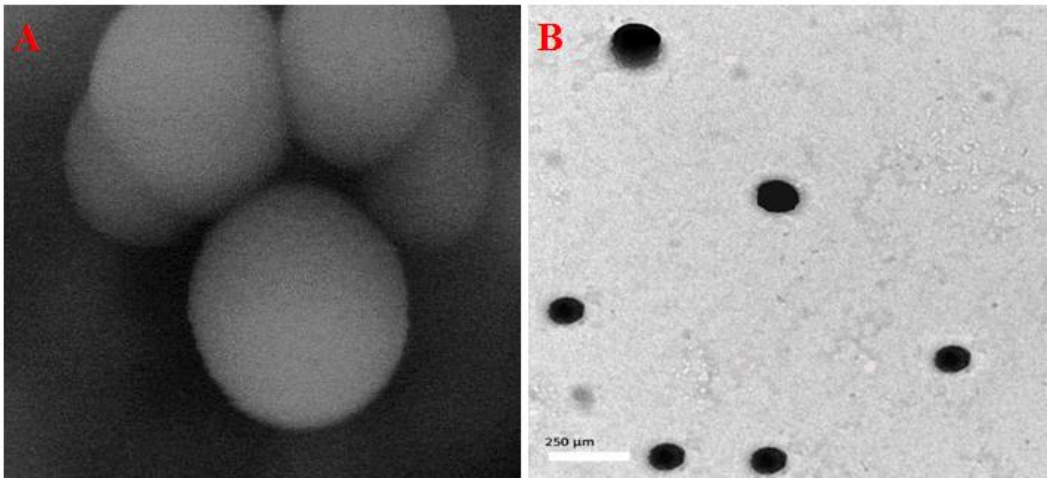

Fig. 8. (A) SEM Photograph of CHMH2 nanoparticles in 50 nm scale. (B) TEM image of CHMH2 nanoparticles in 250 nm scale.

was released from HPMC-xanthan-nanoparticles (CHMX1, CHMX2 and CHMX3) was about 70% after 8 h, while the formulas containing xanthan (CX1, CX2, and CX3) released ≤ 73% within 8 h.

By comparing the physicochemical and functional properties of the prepared nanoparticles (as discussed above), the CHMH2 formulation showed highly advanced results for application in pharmaceutical and drug release applications. In this regard, the CHMH2 exhibited good zeta potential values, smaller and uniform particle sizes, high drug loading and entrapment efficiency. Therefore, the CHMH2 formulation was chosen for further characterization studies. For this purpose, the SEM and TEM studies were performed on the optimized CHMH2 formula, and results are depicted in Fig. 8. From the SEM image, it is clear that the chosen CHMH2 formulation exhibits nano-scale size and spherical particles with smooth surfaces and some agglomeration at the field scale of 250 nm. These results highlight the suitable dimensions and morphology of the prepared nanoparticles. On the other hand, the TEM image of CHMH2 nanoparticles confirmed the SEM results by depicting similar morphology with a core and shell structure without any agglomeration.

Despite many therapeutical effects of Cloperastine hydrochloride, such as antitussive, antiedemic, ntihistaminic, and papaverine-like activity, there have been no trials to formulate this drug into prolonged-release formulations. However, as in our study, some studies were conducted to prepare controlled-release matrices using HPMC and HPC with different drugs. For instance, Shah A et al. formulated enalapril maleate sustained-release matrices using HPMC and HPC. The sustained release tablets of enalapril maleate are accomplished through direct compression utilizing HPMC K15, HPMC K100, and HPC.

polymers alone or in mixture. The drug release investigation of the prepared matrices in phosphate buffer solution (pH 6.8) using USP dissolving equipment II for 24 h hours revealed that all polymer matrices exhibited a protracted release profile individually or in the composite form [49]. In addition, Samie M. et al. developed sustained-release formulations of levosulpiride by direct compression utilizing several cellulose polymers, such as NaCMC, HPC, and HPMC in varying ratios to extend the drug's release. All formulations were evaluated for their in vitro release in a pH 6.8 buffer. The results revealed the release of levosulpiride from the matrix tablet was prolonged, with the retardation sequence being NaCMC > HPC > HPMC. In this regard, the NaCMC was the best-extending polymer among the other polymers, which exhibited the best sustained-release behavior between 9 formulations [50]. Regarding the results of these studies, the prepared formulations in the present study showed suitable physiochemical and functional characteristics for pharmaceutical applications. Among all studied formulations, the CHMH2 formulation showed highly effective

CC BY

physicochemical and functional properties in terms of particle size, PDI, zeta potential, drug loading and drug release properties, which could be chosen as an optimum formulation for further evaluation in future studies.

CONCLUSION

In this work, prolonged-release nanoparticles of Cloperastine hydrochloride were successfully prepared using emulsion solvent evaporation. Different formulae were prepared, and the resultant nanoparticles were evaluated using various characterization methods for their physicochemical and functional properties. The best nanoparticle formula was CHMH2, which contained a drug: HPC: HPMC K4M ratio of 200:100:60 in its composition. This formulation showed proper zeta potential, particle size, and PDI values of -19.54 ± 0.03, 25.47 ± 0.29, and 0.52 ± 0.01, respectively, indicating its nanoscale size and stable nanoparticulate characteristics. Investigation of the production yield, drug loading, and drug release behavior of the formulations showed higher efficiency for all formulations, with the highest values obtained for CHMH2 formulation. Furthermore, the CHMH2 formulation showed 83.02 ± 0.21 of production yield, 89.50 ± 0.19 of %DL, and 84.12 ± 0.22 of %EE. Evaluation of the drug release behavior of the fabricated formulations revealed a two-stage release profile for all formulations. Among the various nanoparticles with different compositions, the xanthan gum-containing formulations produced a more retarded and prolonged release profile than other formulations. The fabricated nanoparticles liberated more than 80% of Cloperastine hydrochloride after 8 hours and prolonged its release for 24 h. Therefore, the individual and composite nanoparticles of natural polymers in the studied ratio in this study could control the release of Cloperastine hydrochloride and could be used for controlled release drug delivery of Cloperastine hydrochloride for 24 h. However, additional studies are required to evaluate the *in vitro* and *in vivo* performance of the fabricated Cloperastine hydrochloride-containing nanoparticles for application in the pharmaceutical filed.

CONFLICT OF INTEREST

The authors declare that there is no conflict of interests regarding the publication of this manuscript.

REFERENCES

1. Yang LL, Yang T. Pulmonary rehabilitation for patients with coronavirus disease 2019 (COVID-19). Chronic Diseases and Translational Medicine. 2020;6(2):79-86.
2. Abazari M, Badeleh SM, Khaleghi F, Saeedi M, Haghi F. Fabrication of silver nanoparticles-deposited fabrics as a potential candidate for the development of reusable facemasks and evaluation of their performance. Sci Rep. 2023;13(1).
3. Cuzzocrea S, Catania M. Pharmacological and clinical overview of cloperastine in treatment of cough. Ther Clin Risk Manag. 2011:83.
4. Jose Luis T. Natural Experiments that Allow to Study Potential Drugs in Coronavirus Disease 2019 (COVID-19) from the General Practice Level. Archives of Family Medicine and General Practice. 2020;5(1).
5. Lobo-Galo N, Gálvez-Ruíz J-C, Balderrama-Carmona AP, Silva-Beltrán NP, Ruiz-Bustos E. Recent biotechnological advances as potential intervention strategies against COVID-19. 3 Biotech. 2021;11(2).
6. Li B, Yu Y, Jiang Y, Zhao L, Li A, Li M, et al. Cloperastine inhibits esophageal squamous cell carcinoma proliferation in vivo and in vitro by suppressing mitochondrial oxidative phosphorylation. Cell Death Discovery. 2021;7(1).
7. Liu H-Y, Cheng Q-Z, Fu H-Z, Zhong Z-H, Xia H-Y, Guo Y-F, et al. Identification and quantification of five impurities in cloperastine hydrochloride. Journal of Pharmaceutical and Biomedical Analysis. 2021;193:113731.
8. Li H, Zhang C, Wang J, Jiang Y, Fawcett JP, Gu J. Simultaneous quantitation of paracetamol, caffeine, pseudoephedrine, chlorpheniramine and cloperastine in human plasma by liquid chromatography–tandem mass spectrometry. Journal of Pharmaceutical and Biomedical Analysis. 2010;51(3):716-722.
9. Kawaura K, Ogata Y, Inoue M, Honda S, Soeda F, Shirasaki T, et al. The centrally acting non-narcotic antitussive tipepidine produces antidepressant-like effect in the forced swimming test in rats. Behav Brain Res. 2009;205(1):315-318.
10. Gao L-C, Luo H-Y, Long H-Z, Zhou Z-W, Xu S-G, Li F-J, et al. Pharmacokinetics, Bioequivalence and Safety of Cloperastine in Chinese Healthy Subjects under the Fasting and Postprandial Conditions. Research Square Platform LLC; 2022.
11. Hoffman A. Pharmacodynamic aspects of sustained release preparations. Adv Drug Del Rev. 1998;33(3):185-199.
12. Hirabayashi H, Takahashi T, Fujisaki J, Masunaga T, Sato S, Hiroi J, et al. Bone-specific delivery and sustained release of diclofenac, a non-steroidal anti-inflammatory drug, via bisphosphonic prodrug based on the Osteotropic Drug Delivery System (ODDS). Journal of Controlled Release. 2001;70(1-2):183-191.
13. Abazari M, Ghaffari A, Rashidzadeh H, Momeni badeleh S, Maleki Y. Current status and future outlook of nano-based systems for burn wound management. Journal of Biomedical Materials Research Part B: Applied Biomaterials. 2019;108(5):1934-1952.
14. Babu A, Templeton AK, Munshi A, Ramesh R. Nanodrug Delivery Systems: A Promising Technology for Detection, Diagnosis, and Treatment of Cancer. AAPS PharmSciTech.

CC BY

2014;15(3):709-721.
15. Deng Y, Zhang X, Shen H, He Q, Wu Z, Liao W, et al. Application of the Nano-Drug Delivery System in Treatment of Cardiovascular Diseases. Frontiers in Bioengineering and Biotechnology. 2020;7.
16. Wilczewska AZ, Niemirowicz K, Markiewicz KH, Car H. Nanoparticles as drug delivery systems. Pharmacol Rep. 2012;64(5):1020-1037.
17. de J. Drug delivery and nanoparticles: Applications and hazards. International Journal of Nanomedicine. 2008:133.
18. Rashidzadeh H, Tabatabaei Rezaei SJ, Adyani SM, Abazari M, Rahamooz Haghighi S, Abdollahi H, et al. Recent advances in targeting malaria with nanotechnology-based drug carriers. Pharmaceutical Development and Technology. 2021;26(8):807-823.
19. Cho K, Wang X, Nie S, Chen Z, Shin DM. Therapeutic Nanoparticles for Drug Delivery in Cancer. Clinical Cancer Research. 2008;14(5):1310-1316.
20. Margalit R. Liposome-Mediated Drug Targeting in Topical and Regional Therapies. Crit Rev Ther Drug Carrier Syst. 1995;12(2-3):233-261.
21. Rashidzadeh H, Mozafari F, Ghaffarlou M, Barsbay M, Ramazani A, Abazari M, et al. Harnessing the Power of Nanomaterials to Alleviate Tumor Hypoxia in Favor of Cancer Therapy. Harnessing Materials for X-ray Based Cancer Therapy and Imaging: Springer International Publishing; 2022. p. 135-174.
22. Mozafari F, Rashidzadeh H, Barsbay M, Ghaffarlou M, Salehiabar M, Ramazani A, et al. Application of Nanoradioprotective Agents in Cancer Therapy. Harnessing Materials for X-ray Based Cancer Therapy and Imaging: Springer International Publishing; 2022. p. 175-200.
23. Kumari A, Yadav SK, Yadav SC. Biodegradable polymeric nanoparticles based drug delivery systems. Colloids Surf B Biointerfaces. 2010;75(1):1-18.
24. Crucho CIC, Barros MT. Polymeric nanoparticles: A study on the preparation variables and characterization methods. Materials Science and Engineering: C. 2017;80:771-784.
25. Mozafari F, Rashidzadeh H, Ghaffarlou M, Salehiabar M, Ertas YN, Ramazani A, et al. ROS-Based Cancer Radiotherapy. Harnessing Materials for X-ray Based Cancer Therapy and Imaging: Springer International Publishing; 2022. p. 265-309.
26. Desgouilles S, Vauthier C, Bazile D, Vacus J, Grossiord J-L, Veillard M, et al. The Design of Nanoparticles Obtained by Solvent Evaporation: A Comprehensive Study. Langmuir. 2003;19(22):9504-9510.
27. Lee M, Cho YW, Park JH, Chung H, Jeong SY, Choi K, et al. Size control of self-assembled nanoparticles by an emulsion/solvent evaporation method. Colloid Polym Sci. 2005;284(5):506-512.
28. Liu D, Jiang S, Shen H, Qin S, Liu J, Zhang Q, et al. Diclofenac sodium-loaded solid lipid nanoparticles prepared by emulsion/solvent evaporation method. J Nanopart Res. 2010;13(6):2375-2386.
29. Abazari M, Jamjah R, Abdollahi H. Investigation of Optimal Condition of Ethylene Polymerization Using a New Three-Metallic High-Performance Ziegler–Natta Catalyst: Experimental Design and Polymer Characterization. Catal Lett. 2022;153(2):622-633.
30. Ekambaram P, Abdul Hasan Sathali A. Formulation and Evaluation of Solid Lipid Nanoparticles of Ramipril. J Young Pharm. 2011;3(3):216-220.
31. Eltawela S. PREPARATION AND CHARACTERIZATION OF (−)-EPIGALLOCATECHIN GALLATE LIPID BASED NANOPARTICLES FOR ENHANCING AVAILABILITY AND PHYSICAL PROPERTIES. Al-Azhar Journal of Pharmaceutical Sciences. 2021;63(1):17-36.
32. Ku Aizuddin KA, Foo Chit S, Gurmeet Kaur Surindar S, Meor Mohd Redzuan MMA. Physicochemical characterization of astaxanthin-loaded PLGA formulation via nanoprecipitation technique. Journal of Applied Pharmaceutical Science. 2020.
33. Kim DW, Yousaf AM, Li DX, Kim JO, Yong CS, Cho KH, et al. Development of RP-HPLC method for simultaneous determination of docetaxel and curcumin in rat plasma: Validation and stability. Asian Journal of Pharmaceutical Sciences. 2017;12(1):105-113.
34. Badran MM, Alomrani AH, Harisa GI, Ashour AE, Kumar A, Yassin AE. Novel docetaxel chitosan-coated PLGA/PCL nanoparticles with magnified cytotoxicity and bioavailability. Biomedicine & Pharmacotherapy. 2018;106:1461-1468.
35. Bayoumi AA. "Enhancement of solubility of a poorly soluble antiplatelet aggregation drug by cogrinding technique". Asian Journal of Pharmaceutical and Clinical Research. 2018;11(10):340.
36. Borman P, Elder D. Q2(R1) Validation of Analytical Procedures. ICH Quality Guidelines: John Wiley & Sons, Inc.; 2017. p. 127-166.
37. Faddis MO, Committee on National F. The Pharmacopoeia of the United States of America. The American Journal of Nursing. 1943;43(2):235.
38. Bales BL. A Definition of the Degree of Ionization of a Micelle Based on Its Aggregation Number. The Journal of Physical Chemistry B. 2001;105(29):6798-6804.
39. Ahmed MM, Ameen MSM, Abazari M, Badeleh SM, Rostamizadeh K, Mohammed SS. Chitosan-decorated and tripolyphosphate-crosslinked pH-sensitive niosomal nanogels for Controlled release of fluoropyrimidine 5-fluorouracil. Biomedicine & Pharmacotherapy. 2023;164:114943.
40. Abazari M, Akbari T, Hasani M, Sharifikolouei E, Raoufi M, Foroumadi A, et al. Polysaccharide-based hydrogels containing herbal extracts for wound healing applications. Carbohydr Polym. 2022;294:119808.
41. Busch W, Bastian S, Trahorsch U, Iwe M, Kühnel D, Meißner T, et al. Internalisation of engineered nanoparticles into mammalian cells in vitro: influence of cell type and particle properties. J Nanopart Res. 2010;13(1):293-310.
42. Kunii R, Onishi H, Machida Y. Preparation and antitumor characteristics of PLA/(PEG-PPG-PEG) nanoparticles loaded with camptothecin. Eur J Pharm Biopharm. 2007;67(1):9-17.
43. Mousazadeh N, Gharbavi M, Rashidzadeh H, Nosrati H, Danafar H, Johari B. Anticancer evaluation of methotrexate and curcumin-coencapsulated niosomes against colorectal cancer cell lines. Nanomedicine. 2022;17(4):201-217.
44. Gharbavi M, Johari B, Mousazadeh N, Rahimi B, Leilan MP, Eslami SS, et al. Hybrid of niosomes and bio-synthesized selenium nanoparticles as a novel approach in drug delivery for cancer treatment. Mol Biol Rep. 2020;47(9):6517-6529.
45. Gharbavi M, Johari B, Rismani E, Mousazadeh N, Taromchi AH, Sharafi A. NANOG Decoy Oligodeoxynucleotide–Encapsulated Niosomes Nanocarriers: A Promising Approach to Suppress the Metastatic Properties of U87

CC BY

Human Glioblastoma Multiforme Cells. ACS Chem Neurosci. 2020;11(24):4499-4515.
46. Ruckmani K, Sankar V. Formulation and Optimization of Zidovudine Niosomes. AAPS PharmSciTech. 2010;11(3):1119-1127.
47. Joseph E, Singhvi G. Multifunctional nanocrystals for cancer therapy: a potential nanocarrier. Nanomaterials for Drug Delivery and Therapy: Elsevier; 2019. p. 91-116.
48. Tantra R, Schulze P, Quincey P. Effect of nanoparticle concentration on zeta-potential measurement results and reproducibility. Particuology. 2010;8(3):279-285.
49. Murtaza G, Ullah H, Khan SA, Mir S, Khan AK, Nasir B, et al. Formulation and In vitro Dissolution Characteristics of Sustained-Release Matrix Tablets of Tizanidine Hydrochloride. Tropical Journal of Pharmaceutical Research. 2015;14(2):219.
50. Savaşer A, Özkan Y, Işımer A. Preparation and in vitro evaluation of sustained release tablet formulations of diclofenac sodium. Il Farmaco. 2005;60(2):171-177.

CC BY